2006

Influence of Processing Parameters on Texture and Microstructure in Aluminum after ECAP

Zhilyaev, A.P.; Oh-ishi, K.; Raab, G.I.; McNelley, T.R.

Trans Tech Publications

Zhilyaev, Alexandre P., et al. "Influence of processing parameters on texture and microstructure in aluminum after ECAP." Materials Science Forum. Vol. 503. Trans Tech Publications, 2006.

https://hdl.handle.net/10945/62625

Materials Science Forum
ISSN: 1662-9752, Vols. 503-504, pp 65-70
doi:10.4028/www.scientific.net/MSF.503-504.65

Online: 2006-01-15

INFLUENCE OF PROCESSING PARAMETERS ON TEXTURE AND MICROSTRUCTURE IN ALUMINUM AFTER ECAP

A. P. Zhilyaev[1, 2, a], K. Oh-ishi[1, b], G. I. Raab[3,c] and T. R. McNelley[1, d]
[1] Department of Mechanical & Astronautical Engineering, Naval Postgraduate School, 700 Dyer Road, Monterey, CA 93943-5146 USA
[2] Institute of Mechanics, Russian Academy of Science, Ufa, 450000 Russia
[3] Institute for Physics of Advanced Materials, USATU, 450000 Russia
[a] apzhilya@nps.edu, [b] koishi@nps.edu, [c] raab@mail.rb.ru, [d] tmcnelley@nps.edu

Keywords: Equal Channel Angular Pressing, Aluminum, Microtexture, Grain refinement, Orientation Imaging Microscopy

Abstract. The influence of strain path during equal-channel angular pressing (ECAP) has been evaluated in pure aluminum by orientation imaging microscopy (OIM) and transmission electron microscopy (TEM). The material was examined after four pressing operations by route B_C in a 90° die, or eight pressing operations by route B_C in a 135° die. The von Mises equivalent strains were essentially the same for these two ECAP procedures. The microtexture data indicate that the distortion during ECAP corresponds to a simple shear in a direction approximately parallel to die-channel exit and on a plane perpendicular to the flow plane. For both procedures the OIM data reveal prominent meso-scale band-like features. Lattice orientations in each band correspond to a texture orientation but the particular combinations of orientations depend upon ECAP die angle. High-angle boundaries in the structure correspond to interfaces between the bands.

Introduction

ECAP is advantageous in producing of ultrafine-grained (UFG) structures in bulk material because the procedure may be applied repeatedly to a billet without changing its cross section [1]. This is in contrast to other methods, such as high-pressure torsion (HPT) [2] and accumulative roll-bonding (ARB) [3]. The applicability to bulk material of still other methods, such as friction stir processing (FSP) [4], must still be established. Although the first publications on ECAP appeared almost 25 years ago [5] in the last decade there has been a surge of interest in the development of UFG structures in pure metals and alloys by this method. A survey of the literature reveals that most publications have been concerned with the capability of ECAP to produce highly refined grains in a range of industrially important materials. The roles of ECAP parameters (die-channel angle, the number of pressing passes, billet rotation between passes and relief angles in the die) in grain refinement have been of primary interest. In general, microstructure refinement and texture evolution during ECAP have been studied separately and few systematic investigations have been conducted on the concomitant development of texture and microstructure.

The strain state during an ECAP pass depends strongly on the die angle. Band-like arrangements of characteristic texture orientations have been reported in the microstructure of pure aluminum processed by repetitive ECAP using a 90° die [6]. Recently, texture measurements after one ECAP pass through a 90° die for pure aluminum [7], pure copper [8] and pure aluminum again [9] have shown that simple shear tends to occur on a plane perpendicular to the flow plane and with shear direction *nearly parallel* to the axis of the die exit channel. These observations are in disagreement with the usual interpretation of the strain state associated with ECAP processing, which assumes that shear occurs on the plane of the die channel intersection in the direction of the *bisector of the die angle*.

The role of the die angle in microstructure and texture development has been examined through scanning of large areas by OIM in pure aluminum processed by ECAP using route B_C with a 90° die (4 passes) and a 135° die (8 passes). The development of the textures and band-like arrangements in the resulting microstructures has been analyzed, and the band-to-band disorientations have been evaluated.

Experimental Procedure

Full details of the materials and processes of this work have been given previously [10,11] Briefly, the pure aluminum material (99.99%) was swaged to a rod 10 mm in diameter and 60 mm in length for pressing in the 90º die. The material was cold rolled and billets were machined with dimensions of 10 × 10 × 60 mm^3 for pressing in the 135º die. Prior to ECAP, these materials were given annealing treatments resulting in initial recrystallized grain sizes of ~1 mm. ECAP of the round billets was conducted at room temperature using a die with an angle, Φ, between channels of 90º and having a relief angle, Ψ, of ~20º; the square billets were pressed through a 135º die having a relief angle of ~13º. Using route B_C, samples were repetitively pressed 4 times through the 90° die, denoted here as the 90º sample, and 8 times through the 135° die, i.e., the 135º sample. The accumulated equivalent strain values for each of these processes were calculated using the die-channel and relief angles in equation 1 [12]:

$$\gamma_N = N\left[\cot\left(\frac{\Phi}{2}+\frac{\Psi}{2}\right)+\frac{\Psi}{2}\mathrm{cosec}\left(\frac{\Phi}{2}+\frac{\Psi}{2}\right)\right] \tag{1}$$

The von Mises equivalent strain has often been calculated using the standard relationship $\varepsilon_{vm} = \left(2/\sqrt{3}\right)\gamma$ [12], although this is valid only in the elastic regime. For large plastic strains such as encountered in ECAP, the von Mises equivalent should be calculated using the following equation [13]:

$$\varepsilon_e = \frac{2}{\sqrt{3}}\ln\left(\sqrt{1+\frac{\gamma^2}{4}}+\frac{\gamma}{2}\right) \tag{2}$$

Using equations (1) and (2) with these values of Φ and Ψ gives $\varepsilon_4 = 2.0$ for a 90° die and $\varepsilon_8 = 1.44$ for a 135°. Prior to examination by OIM, samples were, first, mechanically polished and then electropolished in the Buehler Electromet 4 apparatus using a 20% perchloric acid - 80% ethanol electrolyte solution cooled to -25°C. OIM analyses were always conducted on the flow plane. The symmetry of an ECAP billet is monoclinic, and so the senses of the coordinate axes in the flow plane were carefully ascertained. TEM foil preparation has been described previously [11].

Results and Discussion

Fig. 1 shows gray-scale OIM maps and corresponding discrete pole figures that have been highlighted in colors, using a tolerance of 15º, according to the distinct orientations in the texture. Data for aluminum pressed following route B_C are included in (a) for the 90° sample and in (b) for the 135° sample. These microstructures and textures are represented in the flow plane and the insets that are included with the pole figures are aligned to illustrate the orientation of the ECAP dies for these data. Fig. 1 includes coordinate axes for both samples. Thus, the x-y plane is the flow plane and the billets exit their corresponding dies along the –x direction. The shape changes in the flow plane for unit cubes after a single pass through each die are included in Fig. 1. Two distinct texture orientations are apparent in the 90º sample and the shapes of the regions that correspond to these orientations are congruent with the shape of a volume element subjected to a single ECAP pass through a 90º die. In contrast, there are apparently three orientations in the 135º sample. Regions corresponding to these orientations are band-like in nature but are only partly congruent with the shape change of a volume element for this die angle.

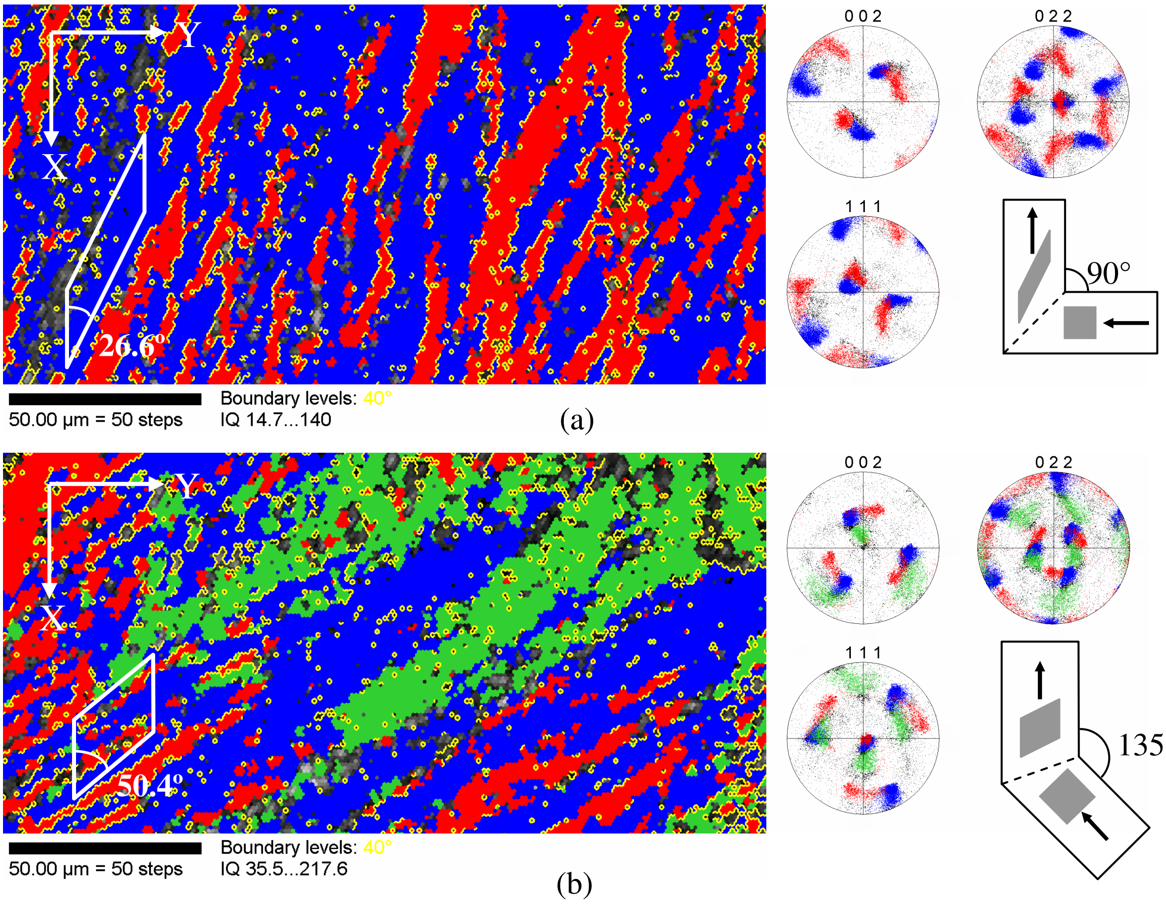

Fig. 1. OIM maps and pole figures for aluminum after (a) 90° sample – four passes (b) 135° sample – eight passes. Gray scale maps and pole figures were highlighted by different colors corresponding to characteristic orientations in the textures. The insets with the pole figures indicate the orientation of the die sets relative to the sample coordinates.

For the 90º sample a traverse was made along a line inclined at ~63.4º to the x axis and the corresponding point-to-origin disorientation distribution is shown in Fig. 2(a); a similar traverse was made for the 135º sample, but at an angle of ~39.6º to the x axis. This result is included in Fig. 2(b). In both cases, these traverses are approximately normal to a set of boundaries between texture orientations. Inspection of these disorientation profiles shows that the difference in lattice orientation across boundaries has a range of 45 - 50° for 90° sample and about 30° for 135° sample.

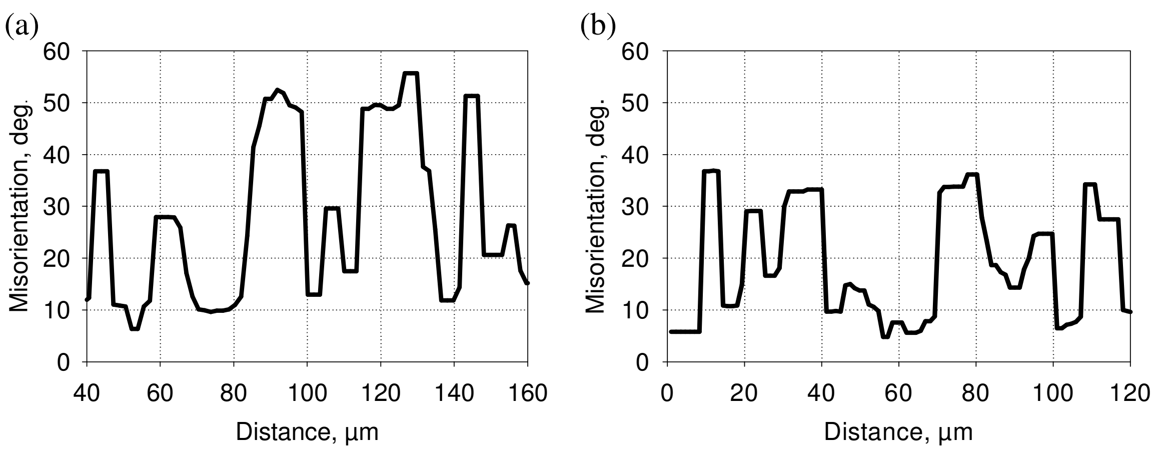

Fig. 2. Point-to-origin disorientation profiles for ECAP aluminum processed by route B_C: (a) the 90° sample – four passes; and (b) the 135° sample – eight passes.

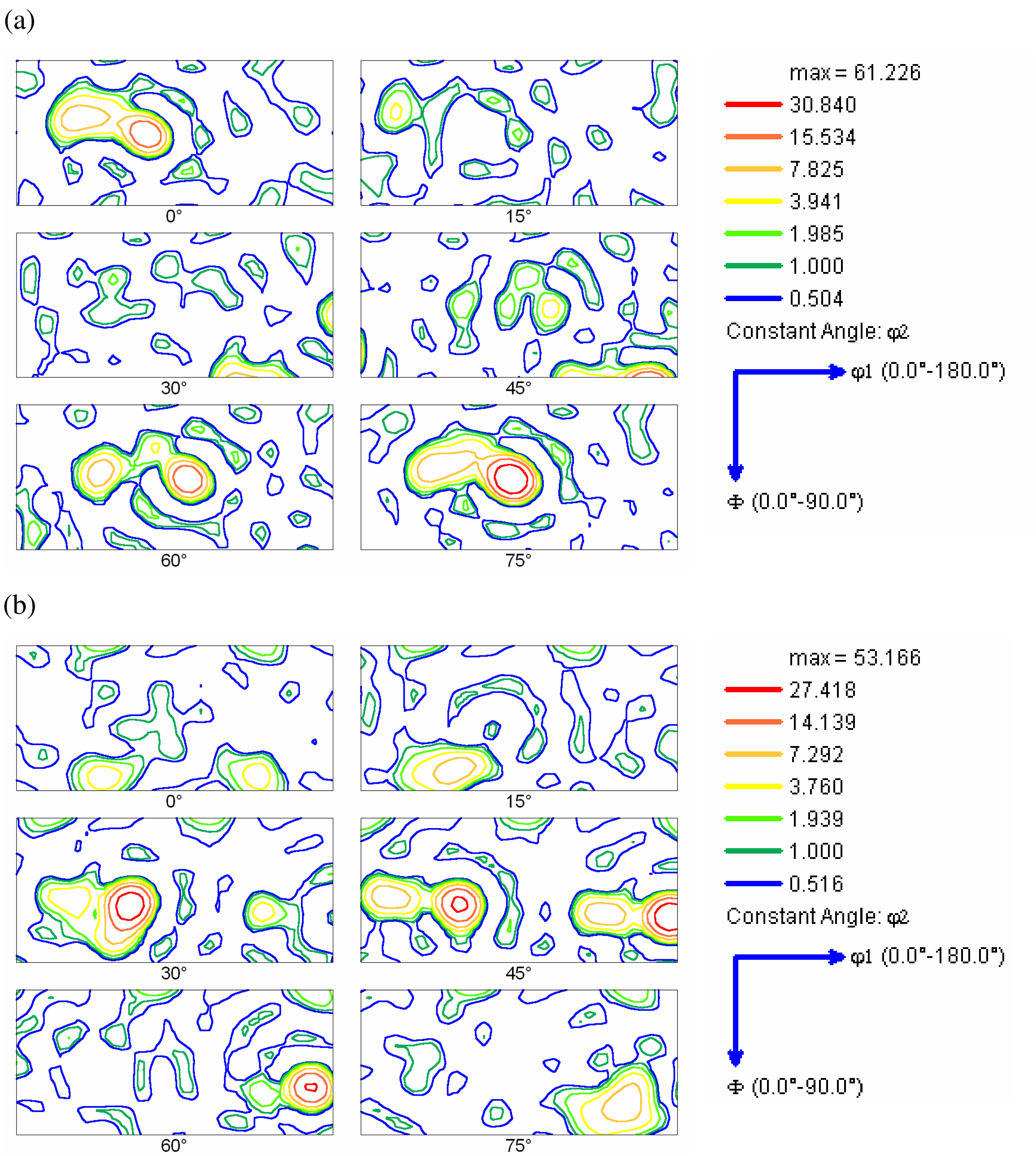

Fig. 3 3D ODFs for ECAP aluminum processed by route B_C: (a) the 90° sample – four passes; (b) the 135° sample – eight passes.

Boundaries of disorientation ≥40º are highlighted in yellow in Fig. 1 and it is apparent that there are more of these boundaries in the 90º sample.
Orientation distribution functions (ODFs) were calculated from the texture data for these samples using Bunge's definition of the Euler angles in relation to the axes indicated in Fig.1. The results are depicted in Fig. 3 where the ODFs are represented by iso-lines. In this representation, φ_1 is a rotation about z (i.e., the flow plane normal), Φ is a rotation about the new x′ axis, and φ_2 is a rotation about the final z″ axis. The fundamental zone of the ODF involves $0º \leq \varphi_1 \leq 180º$ because of the monoclinic symmetry of an ECAP billet [9]. An ECAP pass is often described in terms of a simple shear in the flow plane. Canova, et al. [14] have classified fcc torsion (shear) textures in terms three components: the A fiber, {111}⟨*hkl*⟩, the B-fiber {*hkl*}⟨110⟩ and the C-component {001}⟨110⟩, where the notation refers to {plane parallel to the shear plane}<direction parallel to the shear direction>. In the coordinate system chosen here differences between observed and

Table 1 Prominent texture orientations observed in the 90° and 135° -samples

φ_2	Experiment. orientations	I/I_0	Nearby ideal shear texture components			Δ**	Color
			Type	Euler angles	FP // SP // SD*		
90° sample							
0	35, 35, 0	12	A	35, 45, 0	$(011)//(\bar{1}\bar{1}1)//[2\bar{1}1]$	10	Red
	75, 45, 0	30	C	90, 45, 90	$(011)//(100)//[0\bar{1}1]$	15	Blue
45	120, 90, 45	7	A	125, 90, 45	$(110)//(1\bar{1}1)//[\bar{1}12]$	5	Red
	165, 90, 45	28	C	180, 90, 45	$(110)//(001)//[\bar{1}10]$	15	Blue
75	85, 45, 75	60	B	100, 45, 75	$(414)//(1\bar{8}1)//[\bar{1}01]$	15	Blue
135° sample							
0	51, 81, 0	6	–	–		–	Green
	135, 82, 0	5	–			–	Green
45	15, 50, 45	12	B	0, 54, 45	$(111)//(11\bar{2})//[1\bar{1}0]$	21	Red
	55, 55, 45	33	B	60, 54, 45	$(111)//(2\bar{1}\bar{1})//[0\bar{1}1]$	5	Blue
	140, 60, 45	12	B	120, 54, 45	$(111)//(1\bar{2}1)//[\bar{1}01]$	21	Red
	175, 60, 45	49	B	180, 54, 45	$(111)//(\bar{1}\bar{1}2)//[\bar{1}10]$	8	Blue

* (Flow plane) // (Shear plane) // [Shear direction]

** Deviation from ideal position assuming that shear direction // x-axis, shear plane // (x-z) plane in Fig. 1.

theoretical shear texture components may correspond to translations along φ_1 only, i.e. rotations about the flow plane normal.

The distinct orientations in the observed textures mainly lie near variants of the B fiber in the ODF although the specific texture components differ for these two strain paths. A C-component (located at one end of the B fiber) is also apparent in the 90° sample but does not appear in the 135° sample. The prominent lattice orientations and nearest ideal shear texture components for these samples are summarized in Table 1. In both samples the experimental texture data suggest that the shear direction is more nearly aligned with the axis of the die exit channel rather than with the bisector of the die angle. Disorientations among the prominent orientations were calculated for each sample; the maximum disorientation was 55° about [101] for the 90° sample and 35.5 about [320] for the 135° sample. From these data, use of a 90º die results in texture variants of higher disorientation and thus is more effective in creating high-angle boundaries than use of a 135º die. Fig. 4 shows typical TEM micrographs; these images reveal microstructures having comparable (sub)grain sizes (~1.2 μm) and morphologies in these two samples. At the resolution of TEM there is little difference in microstructure and a similar conclusion can be drawn from another study [10]. Comparison of the dimensional scales in Figs. 1 and 4 reveals that the regions examined by TEM may not include all relevant features of the microstructure.

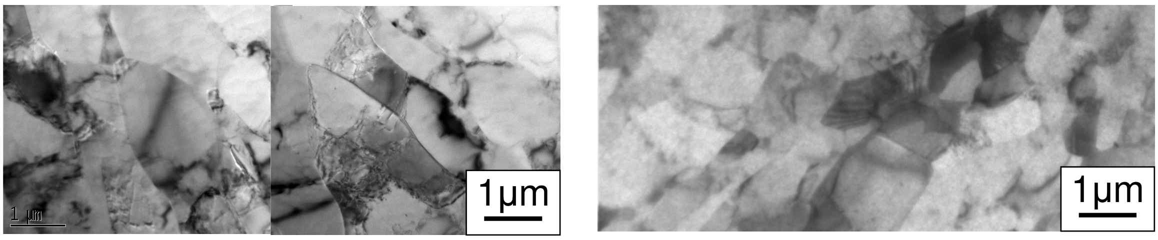

(a) (b)

Fig. 4 TEM images of ECAP (route B_C) aluminum: (a) 90° sample – four passes, and (b) 135º sample – eight passes.

In particular, the distribution of the band- or block-like features apparent at a meso-scale in the OIM data would be difficult to establish by TEM examination alone.

Conclusions

1. Alternating band- or block-like features are apparent in aluminum after four passes through 90º die and eight passes through 135º die by route B_C.
2. Individual bands correspond to characteristic lattice orientations in the texture
3. The band- or block-like features have shapes more or less congruent with the shape change of a volume element as it passes through the die channel intersection.
4. Disorientations between these features are high angle boundaries (up to 55° for the 90° sample and up to 35° in the 135° sample).
5. From analysis of texture data, the shear plane and shear direction are rotated about the flow plane normal, and are almost parallel to the axis of the die exit channel.

Acknowledgements

The authors acknowledge provision of ECAPed materials by Profs. T.G. Langdon (Univ. of Southern California, Los Angeles) and Z. Horita (Kyushu Univ., Fukuoka, Japan). One of the authors (APZ) thanks the National Research Council of the National Academy of Science (U. S. A.) for financial support.

References

[1] Y.T. Zhu, T.G. Langdon, R.Z. Valiev, S.L. Semiatin, D.H. Shin, and T.C. Lowe (eds.).*Ultrafine Grained Materials III* (TMS, Warrendale, PA 2004)
[2] N.A. Smirnova, V.I. Levit, V.I. Pilyugin, R.I. Kuznetsov, L.S. Davydova, V.A. Sazonova: Fiz. Metal. Metalloved. Vol. 61 (1986), p. 1170.
[3] Y.Saito, H. Utsunomiya, N. Tsuji, T. Sakai: Acta Mater. Vol. 47 (1999), p. 579.
[4] K. Oh-ishi and T.R. McNelley, Metal. Mater. Trans. A, 35A (2004) 2951.
[5] V.M. Segal, V.I. Reznikov, A.E. Drobyshevskiy, V.I. Kopylov: Russ. Metall. (Metally) Vol. 1 (1981), p. 99.
[6] T.R. McNelley and D.L. Swisher, in Ultrafine Grained Materials III, edited by Y.T. Zhu, T.G. Langdon, R.Z. Valiev, S.L. Semiatin, D.H. Shin, and T.C. Lowe. (TMS, Warrendale, PA, 2004) p. 89.
[7] A. Gholinia, P. Bate and P.B. Prangnell: Acta Mater. Vol. 50 (2002), p. 2121.
[8] L.S. Tóth, R.A. Massion, L. Germain, S.C. Baik and S. Suwas: Acta Mater. Vol. 52 (2004), p. 1885.
[9] D. L. Swisher, K. Oh-ishi, A. P. Zhilyaev, M. R. McNelley: (2004), to be published.
[10] K. Nakashima, Z. Horita, M. Nemoto and T.G. Langdon: Acta mater. Vol. 46 (1998), p. 1589.
[11] S.D. Terhune, D.L. Swisher, K. Oh-ishi, Z. Horita, T.G. Langdon, and T.R. McNelley: Metall. Trans. Vol. 33A (2002), p. 2173.
[12] Y. Iwahashi, J. Wang, Z. Horita, M. Nemoto, T.G. Lengdon: Scripta Mater. Vol. 35 (1996), p. 143.
[13] N. H. Polakowski, E. J. Ripling: *Strength and structure of engineering materials* (Prentice-Hall, Englewood Clifts, NJ, 1966) p.383.
[14] G.R. Canova, U.F. Kocks and J.J. Jonas: Acta metal. Vol. 32 (1984), p. 211.

Nanomaterials by Severe Plastic Deformation

10.4028/www.scientific.net/MSF.503-504

Influence of Processing Parameters on Texture and Microstructure in Aluminum after ECAP

10.4028/www.scientific.net/MSF.503-504.65

DOI References

[4] K. Oh-ishi and T.R. McNelley, Metal. Mater. Trans. A, 35A (2004) 2951.
10.1007/s11661-004-0242-1
[7] A. Gholinia, P. Bate and P.B. Prangnell: Acta Mater. Vol. 50 (2002), p. 2121.
10.1016/S1359-6454(02)00055-1
[11] S.D. Terhune, D.L. Swisher, K. Oh-ishi, Z. Horita, T.G. Langdon, and T.R. McNelley: Metall. Trans. Vol. 33A (2002), p. 2173.
10.1007/s11661-002-0049-x
[12] Y. Iwahashi, J. Wang, Z. Horita, M. Nemoto, T.G. Lengdon: Scripta Mater. Vol. 35 (1996), p. 143.
10.1016/1359-6462(96)00107-8
[14] G.R. Canova, U.F. Kocks and J.J. Jonas: Acta metal. Vol. 32 (1984), p. 211.
10.1016/0001-6160(84)90050-6